

Linear Accelerator Design for the LCLS-II FEL Facility

P. Emma, J. Frisch, Z. Huang, H. Loos, A. Marinelli, T. Maxwell, Y. Nosochkov, T. Raubenheimer, J. Welch, L. Wang, M. Woodley, SLAC, Stanford, CA 94309, USA;
A. Saini, N. Solyak, FNAL, Batavia, IL 60510, USA;
J. Qiang, M. Venturini, LBNL, Berkeley, CA 94720, USA



FEL 2014

ABSTRACT

The LCLS-II is an FEL facility proposed in response to the July 2013 BESAC advisory committee, which recommended the construction of a new FEL light source with a high-repetition rate and a broad photon energy range from 0.2 keV to at least 5 keV. A new CW 4-GeV electron linac is being designed to meet this need, using a superconducting (SC) L-band (1.3 GHz) linear accelerator capable of operating with a continuous bunch repetition rate up to 1 MHz at ~ 16 MV/m. This new 700-m linac is to be built at SLAC in the existing tunnel, making use of existing facilities and providing two separate FELs, preserving the operation of the existing FEL, which can be fed from either the existing copper or the new SC linac. We briefly describe the acceleration, bunch compression, beam transport, beam switching, and electron beam diagnostics. The high-power and low-level RF systems, and cryogenic systems are not covered here.

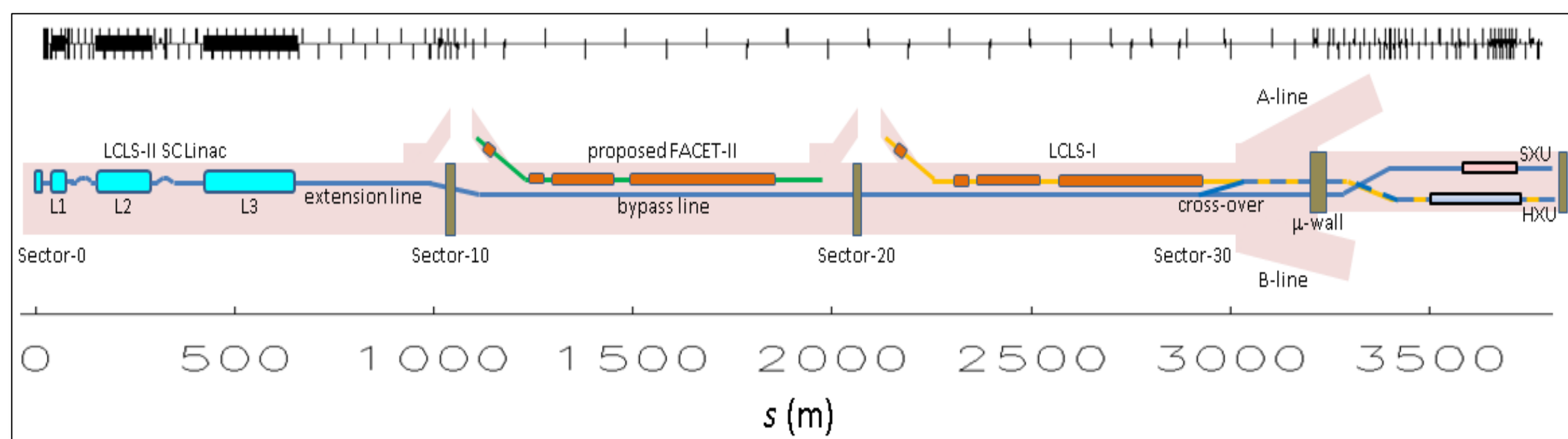


Figure 1: LCLS-II layout in existing SLAC tunnels (3.8 km).

Table 2: Electron Beam Parameters (Nominal and Range)

Parameter	sym.	nom.	range	unit
Final energy	E_f	4.0	2.0-4.1	GeV
Bunch charge	Q_b	100	10-300	pC
CW linac bunch rate	f_b	0.62	0-0.93	MHz
Avg. linac current	I_{av}	62	1-300	μ A
Avg. linac e^- power	P_{av}	0.25	0-1.2	MW
Emittance (norm., x & y)	$\gamma\epsilon_{L-x}$	0.45	0.2-0.7	μ m
Final peak current	I_{pk}	1.0	0.5-1.5	kA
Final rms bunch length	σ_z	8.6	0.6-52	μ m
Compression factor*	C_T	85	25-150	-
Final slice E-spread, rms	σ_{Ez}	500	125-1500	keV

* Total magnetic, from injector-end (100 MeV) to undulator.

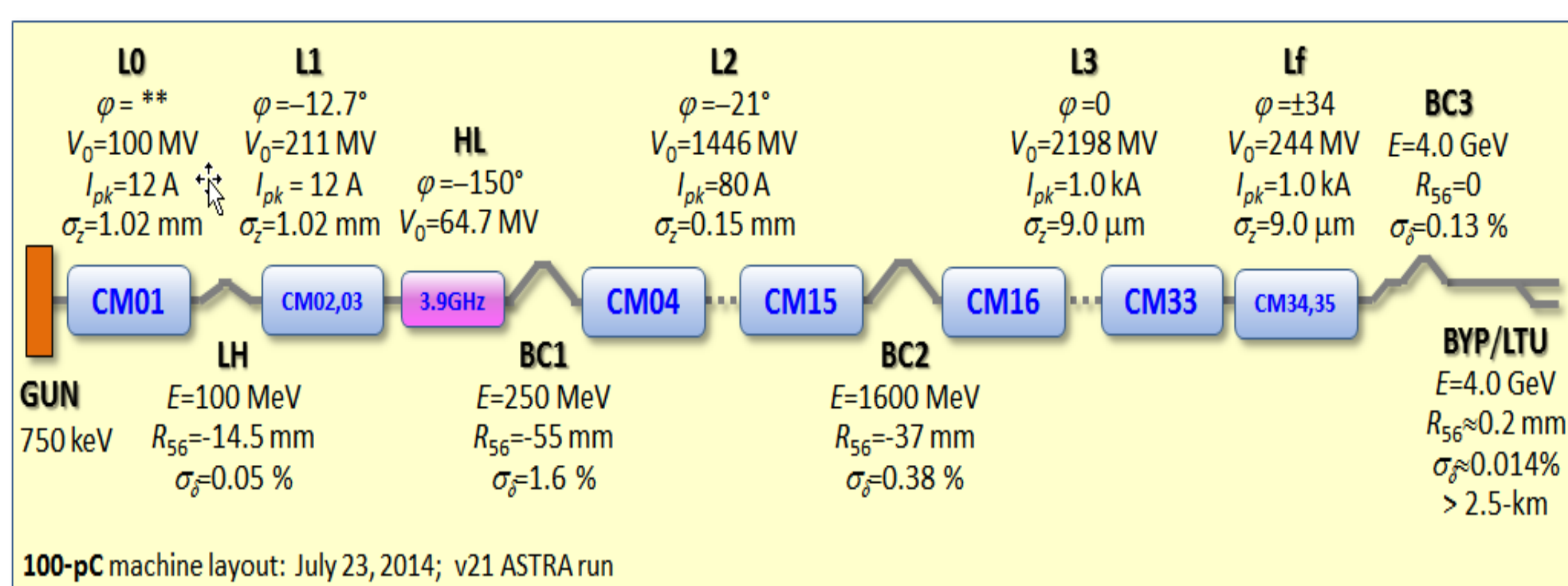


Figure 2: Linac layout with RF and compression parameters. Most RF gradients are held at less than 16 MV/m, the HL section is a 3.9-GHz linac, and LH is the laser heater.

Table 1: SC-linac RF Parameters at 100 pC/bunch

Linac section	Phase (deg)	Gradient (MV/m)	No. of CM's	Avail. cavities	Powered cavities
L0	~ 0	16.3	1	8	7
L1	-12.7	13.6	2	16	15
HL	-150	12.5	2	16	15
L2	-21	15.5	12	96	90
L3	0	15.7	18	144	135
Lf	± 34	15.7	2	16	15

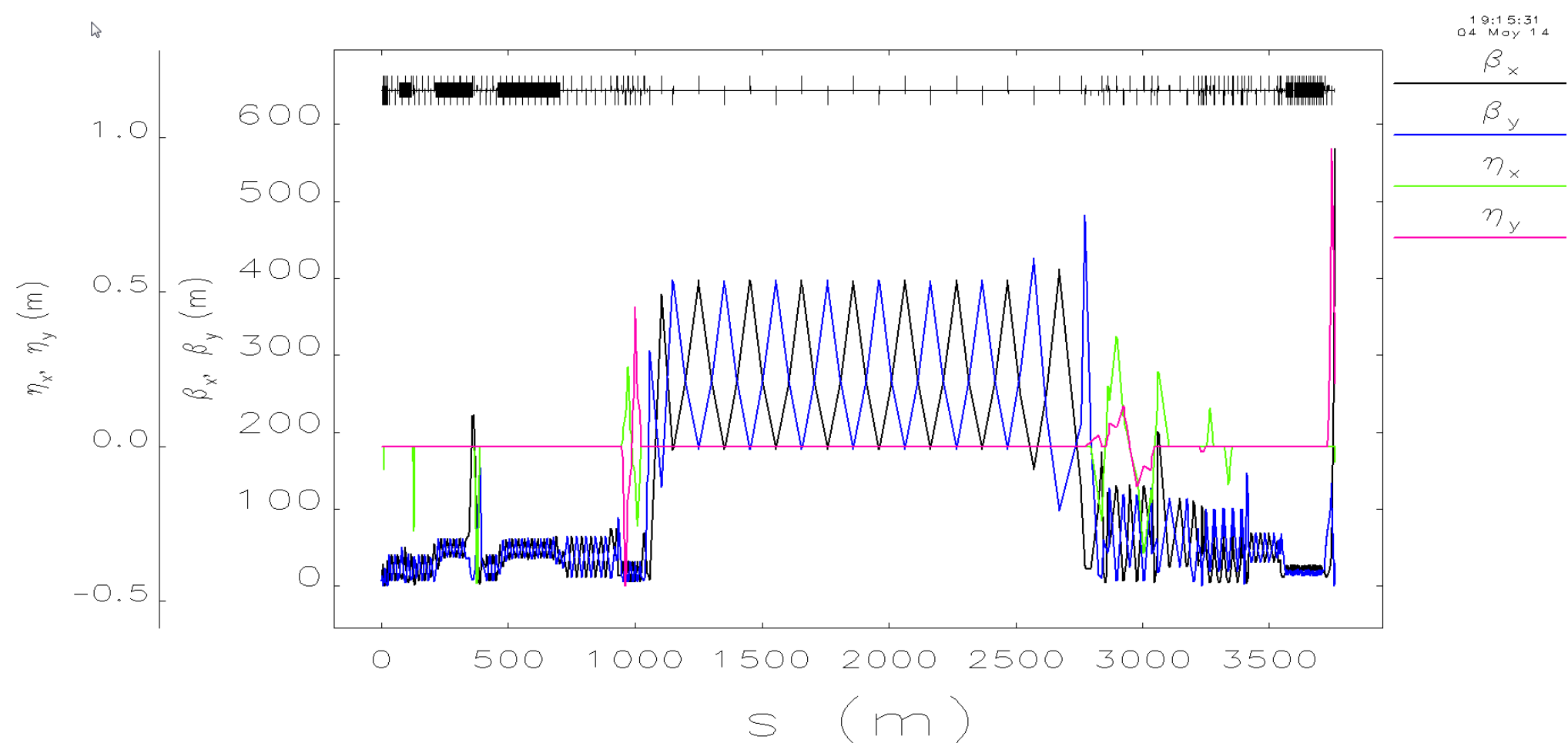


Figure 3: Focusing lattice from cathode to HXR dump. Large beta functions are in the existing, long bypass line, while the HXR undulator is near the end of the line at $s \approx 3550-3700$ m.

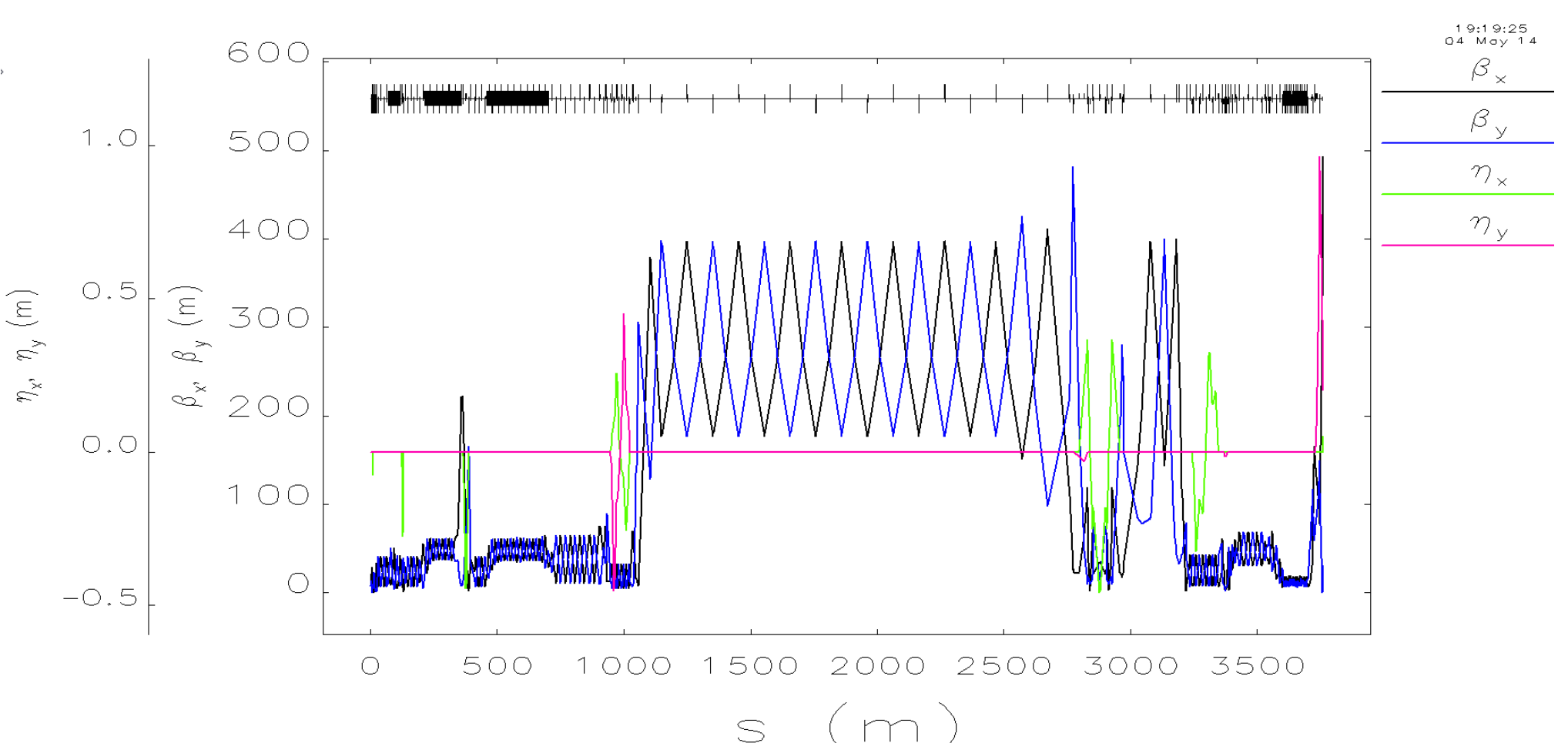


Figure 4: Focusing lattice from cathode to SXR dump at 4 GeV. The SXR undulator is near the end of the line at $s \approx 3600-3700$ m. The two lines split (to HXR or SXR) at $s \approx 2776$ m.

Table 3: Longitudinal Stability Tolerances at 100 pC/bunch

Parameter (rms)	symbol	Tol.	N cav's	unit
Phase error in L0	$\Delta\phi_0$	0.040	7	degL
Phase error in L1	$\Delta\phi_1$	0.039	15	degL
Phase error in HL	$\Delta\phi_H$	0.039	15	degH
Phase error in L2	$\Delta\phi_2$	0.095	90	degL
Phase error in L3-linac	$\Delta\phi_3$	1.8	150	degL
Amplitude error in L0	$\Delta V_0/V_0$	0.026	7	%
Amplitude error in L1	$\Delta V_1/V_1$	0.039	15	%
Amplitude error in HL	$\Delta V_H/V_H$	0.039	15	%
Amplitude error in L2	$\Delta V_2/V_2$	0.095	90	%
Amplitude error in L3	$\Delta V_3/V_3$	0.12	150	%
Laser timing error*	Δt_c	0.31	-	ps
Bunch charge error	$\Delta Q/Q_0$	1.5	-	%
Current reg. in LH	$\Delta I_H/I_H$	0.005	-	%
Current reg. in BC1	$\Delta I_1/I_1$	0.005	-	%
Current reg. in BC2	$\Delta I_2/I_2$	0.003	-	%

* The gun timing error is compressed by 3.85, from gun to 100 MeV, due to velocity compression.

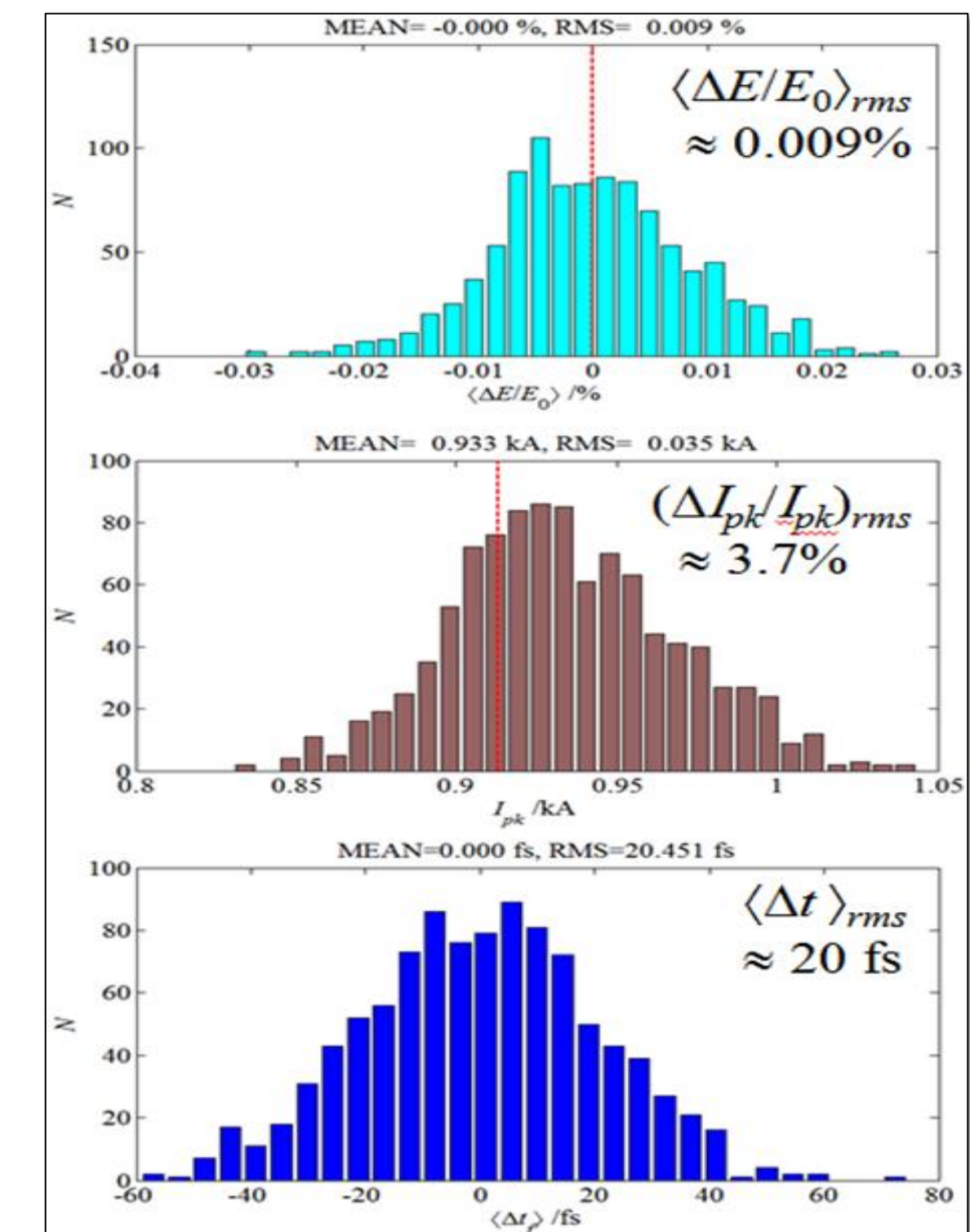


Figure 5: Jitter/tracking simulation using LiTrack and rms (Gaussian) stability tolerances of Table 3, confirming the final expected stability of $(\Delta E/E)_{rms} \approx 0.009\%$, $(\Delta I_{pk}/I_{pk})_{rms} \approx 3.7\%$, and $\Delta t_{rms} \approx 20$ fs rms. It also may be possible to do better.

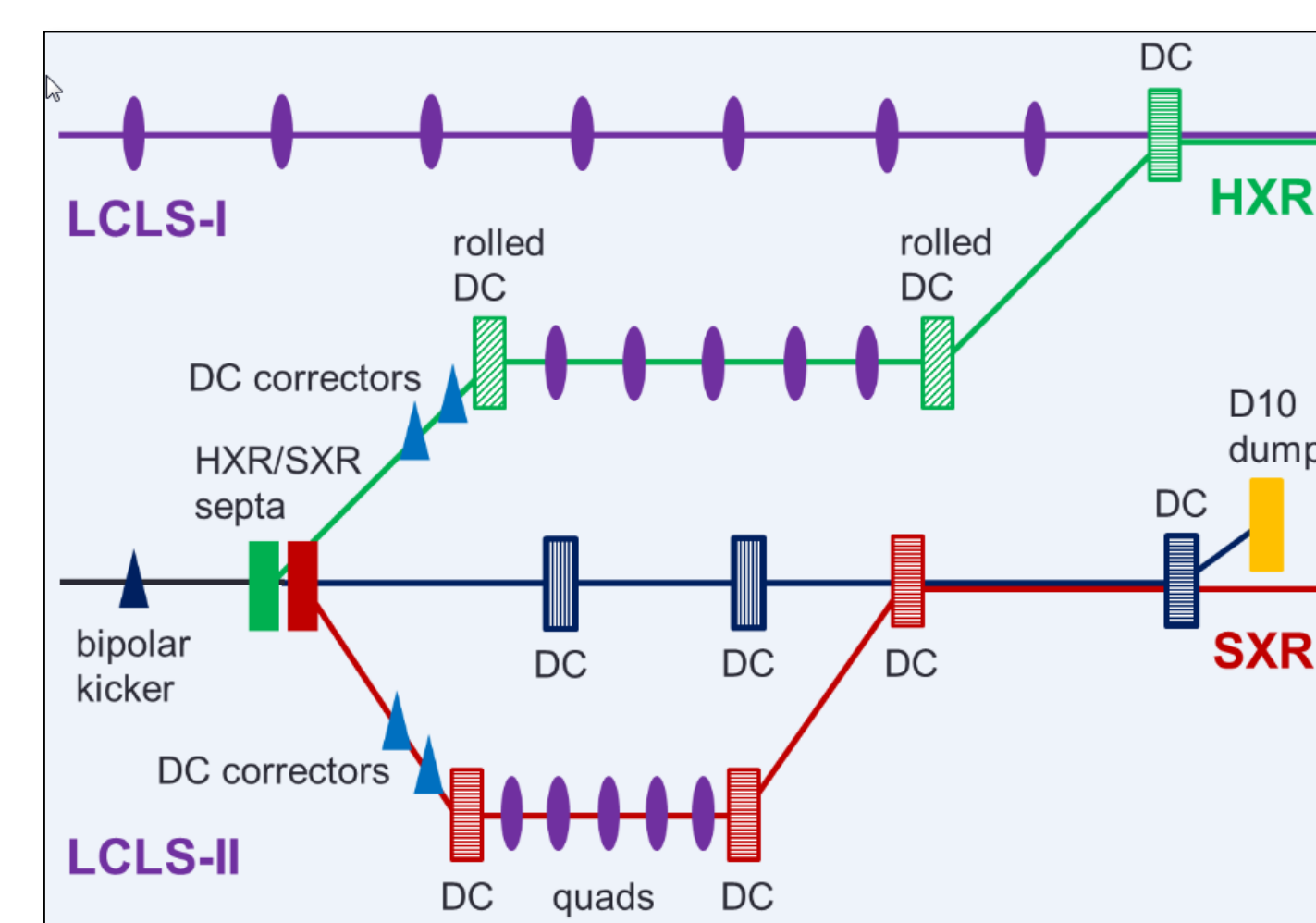


Figure 6: Fast beam spreader system (plan view) with vertical "kicker" and two "2-hole septa" magnets which bend horizontally. This schematic shows the geometry rather than the complete optics (e.g., not all quads are shown here).

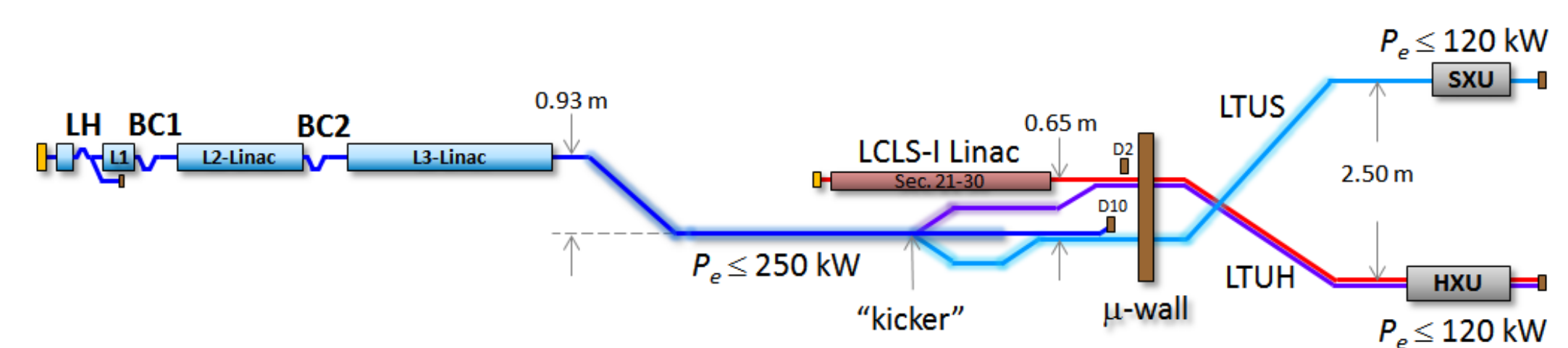


Figure 7: Full LCLS-II layout (plan view) with switching into the SXR undulator (top-right) and HXR undulator (lower-right) at up to a 1-MHz switching rate using a fast "kicker".

Table 4: Resistive-Wall Wakefields of Long Transport

Beamline Section	Pipe Length (m)	Pipe Radius (mm)	Pipe Material	Cond. $(\text{Ohm}\cdot\text{m})^{-1}$
Linac Exten.	250	24.5	stainless	1.37
Dog-Leg #1	78	19	stainless	1.37
Bypass Line	1734	24.5	stainless	1.37
LTU-SXR	827	24.5	Alum.	36.0
LTU-HXR*	778	20.6	Copper	58.0

* Much of this pipe exists and is copper plated to reduce wakes.

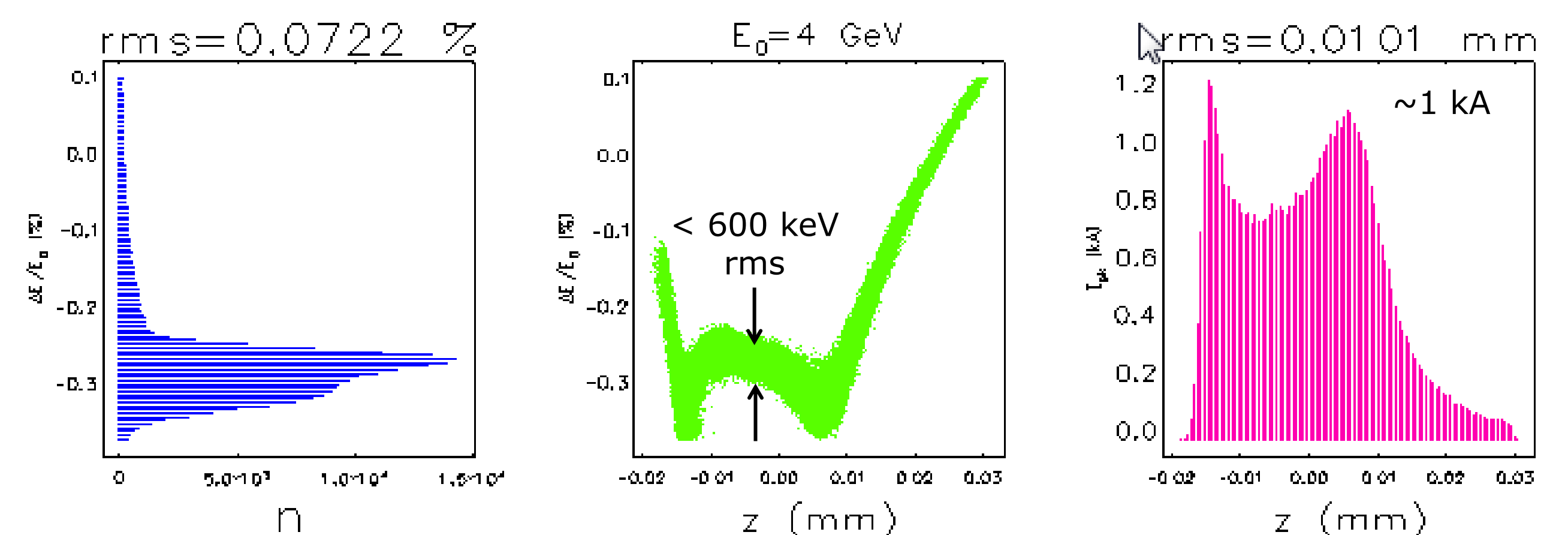


Figure 8: Elegant tracking results of longitudinal phase space (100 pC/bunch) including resistive-wall wakes and CSR in the bends. Space charge is only included in the ASTRA injector tracking. The energy chirp (middle) has been flattened by RW-wall wakefields.

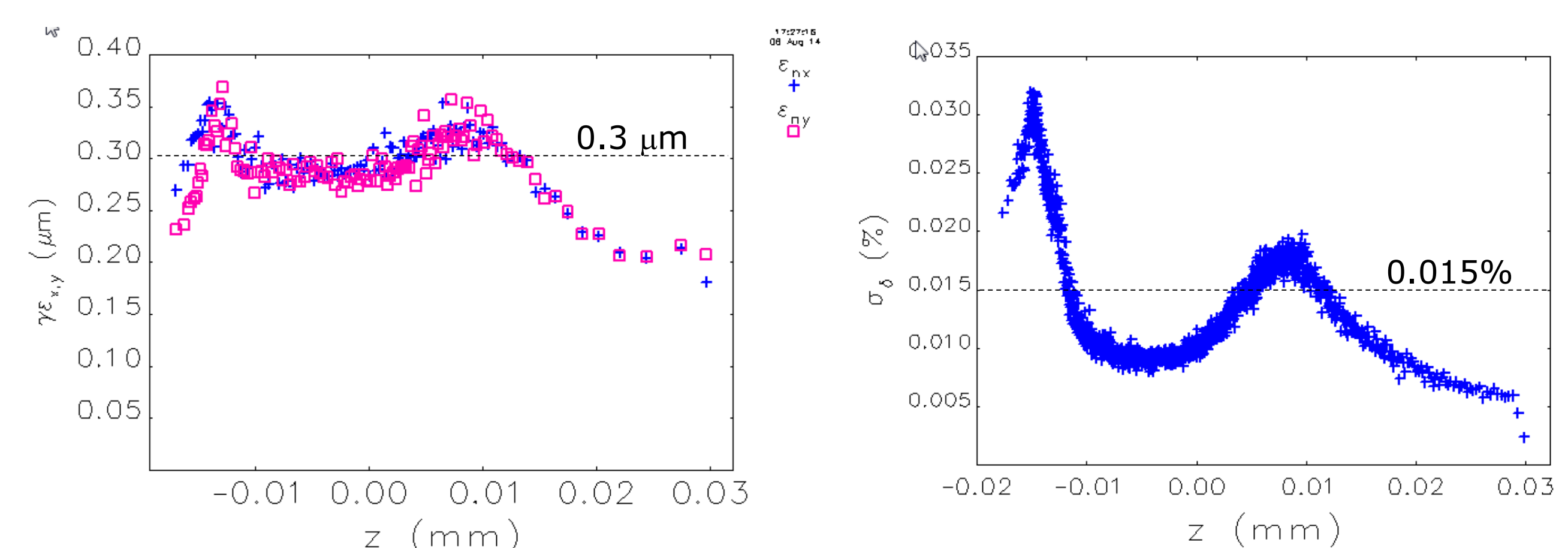


Figure 9: Elegant tracking results showing slice emittance (left) and slice energy spread (right), both within FEL requirements ($\gamma_{e,y} < 0.45 \mu\text{m}$ and $\sigma_{E/E} < 0.015\%$ rms in core).